# Real-space, mean-field algorithm to numerically calculate long-range interactions

A. Cadilhe *, B.V. Costa

*Laboratório de Simulação, Departamento de Física da Universidade Federal de Minas Gerais, 31720-901 Belo Horizonte, Minas Gerais, Brazil*

## HIGHLIGHTS

- A mean-field method to compute long-range interactions in real space is introduced.
- The method describes well the behavior of the anisotropic dipolar Heisenberg model.
- We show that the dipolar interaction is robust to such an approximation.

## ARTICLE INFO

## ABSTRACT

Long-range interactions are known to be of difficult treatment in statistical mechanics models. There are some approaches that introduce a cutoff in the interactions or make use of reaction field approaches. However, those treatments suffer the illness of being of limited use, in particular close to phase transitions. The use of open boundary conditions allows the sum of the long-range interactions over the entire system to be done, however, this approach demands a sum over all degrees of freedom in the system, which makes a numerical treatment prohibitive. Techniques like the Ewald summation or fast multipole expansion account for the exact interactions but are still limited to a few thousands of particles.

In this paper we introduce a novel mean-field approach to treat long-range interactions. The method is based in the division of the system in cells. In the *inner* cell, that contains the particle in sight, the 'local' interactions are computed exactly, the 'far' contributions are then computed as the average over the particles inside a given cell with the particle in sight for each of the remaining cells. Using this approach, the large and small cells limits are exact. At a fixed cell size, the method also becomes exact in the limit of large lattices. We have applied the procedure to the two-dimensional anisotropic dipolar Heisenberg model. A detailed comparison between our method, the exact calculation and the cutoff radius approximation were done. Our results show that the cutoff-cell approach outperforms any cutoff radius approach as it maintains the long-range memory present in these interactions, contrary to the cutoff radius approximation. Besides that, we calculated the critical temperature and the critical behavior of the specific heat of the anisotropic Heisenberg model using our method. The results are in excellent agreement with extensive Monte Carlo simulations using Ewald summation.

© 2015 Elsevier B.V. All rights reserved.

---

* Corresponding author.
  *E-mail addresses:* cadilhe.antonio@gmail.com (A. Cadilhe), bvc@fisica.ufmg.br (B.V. Costa).

## 1. Introduction

Interactions between particles in the physical world are non-local, i.e., they are long ranged. In some important cases the interaction is shielded, so that, considering a few neighbors gives a good description of the system. In general long-range interactions always introduce some complexity in analytical and numerical calculations as well. As a general rule short-ranged interactions are easier to treat numerically. On the other hand Coulomb interactions, for example, are approximated by introducing a cutoff in the potential or using some kind of approach like Ewald summation [1–4] or fast multipole expansion [5,6]. A cutoff is appropriated for disordered systems far from any phase transition or when the interaction decay is fast enough. It has the advantage of preserving the short-range correlations, being of easy numerical implementation, but fails when long-range correlations are important. By considering the Ewald summation, or the fast multipole approach, we exactly account for the long-range interactions, however, the computing time becomes prohibitive as the volume of the system grows. While the cutoff approach allows us to treat millions of particles using a typical desktop computer, the Ewald summation restrict us to a few thousands. In this communication we present a new approach, the *Cutoff-Cell* (*CC*) method, to treat potentials with long-range interactions. As will be discussed in the following it has the benefit of preserving short and long correlations. Intermediate correlations are averaged. It is much better than any cutoff, competing quite well with the exact numerical results. Besides that, the CPU time used in its computation is comparable to that in the cutoff calculation and up to two orders of magnitude shorter than exact calculation. In general, methods to treat long-range potentials divide the interaction in two parts: One, short ranged, non-zero only for separations less than a certain cutoff radius. A second part, is summed in the Fourier space [7,8]. Also, in the present approach we separate the potential in two parts, one short ranged and the other long ranged. However, we do not perform a sum over the long-range term in Fourier space. Instead, we divide the system in sub-domains where the sum in direct space is done. This strategy can be very effectively performed by appropriately choosing the size of the sub-domains. Further improvement to speed up the algorithm is achieved by using tables for the neighbors and potential.

We chose two different models to explain and test how the approach works, respectively. Because of the simplicity of the equations we consider a 'pedagogical model' consisting of $N$ particles in a box of volume $\Omega$ interacting through a Lennard-Jones (6–12) potential. The second example consists of a classical spin model with dipolar interactions. The *CC* method is carefully explained in each case and the approximation for the Hamiltonians are obtained. In the Lennard-Jones case comparing the *CC* approach with other approaches is worthless since the fast decaying of the Lennard-Jones interaction can veil any discrepancy between them. Going a bit further, we apply the *CC* method to the two-dimensional anisotropic dipolar Heisenberg (2*dADH*) model. It is known that this model has at least three well defined phase transition lines. In Refs. [9–11] results using different approaches are reported. To study the long-range dipolar interaction, various methods have been devised, such as the Ewald summation technique [9,10,12–14], the Particle–Particle–Particle-Mesh (P$^3$M) method [7], and the naive cutoff radius method [11,15]. The P$^3$M method is known to give good results in molecular dynamics simulations. Recently some effort has being done to use it in Monte Carlo calculations [16–18]. However, the computer codes are much more difficult to implement than ours. The Ewald summation technique is widely used in Monte Carlo simulations and has been the prime method of choice to study systems with long-range interactions [3,4,9,12–14,19,20]. However, a full implementation is not simple. A crude approximation is to introduce a cutoff radius for the long-range interactions, but this approximation does not work well in dipolar systems [9,10,12,21]. Our novel approximate calculation of the long-range dipolar interaction avoids the drawbacks of the cutoff approximation and becomes exact in the limits of large and small cell sizes as will be discussed in the next section. Using the cutoff-cell method we have simulated the 2dADH model using the single histogram technique. The results we obtained are in excellent agreement with those in literature, showing that the cutoff-cell method is a competitive technique to be used in extensive simulations. As a grateful surprise we observed that the method preserved the critical behavior of the model. Considering the complexity of the interactions studied we dare to say that the same could be expected for more complex systems.

This paper is organized in the following way. In Section 2 we discuss the general principles of the method and in Section 3 we apply the method to the two-dimensional ADHM. In Section 3.2 we present our results for the ADHM in two dimensions and conclude in Section 4.

## 2. The cutoff-cell approach

Let us consider a system of $N$ particles inside a volume $\Omega$ described by a general particle Hamiltonian $\mathcal{H}$. Suppose that $\mathcal{H}$ is separable in two parts, one consisting of short range (*SR*) interactions and the other gathering all long-range (*LR*) ones, $\mathcal{H} = H_{SR} + H_{LR}$

$$H_{SR} = \sum_{\substack{over\ all\ pairs\ |\vec{r}_i - \vec{r}_j| \leq r_0}} h_{SR}(\vec{r}_i, \vec{r}_j)$$

$$H_{LR} = \sum_{All\ pairs} h_{LR}(\vec{r}_i, \vec{r}_j). \tag{1}$$

Here, $r_0$ is the range of the interaction. Numerically, the first term does not represent any problem since the number of arithmetic operations to evaluate it grows linearly with $N$. On the other hand the evaluation of the second term runs over
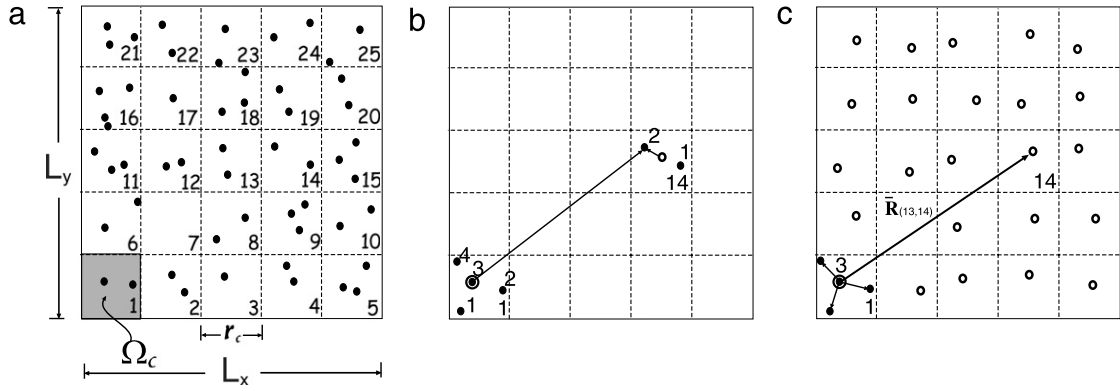
**Fig. 1.** Schematic of an instantaneous realization for a given site $i$ on a two dimensional lattice, $L = L_x = L_y$. Here $\Lambda = 25$. The interaction is exactly calculated for all particles contained within the cell centered on site $i$, $\lambda = 1$, and approximately on the remaining cells.

all pairs of particles such that the number of arithmetic operations needed to evaluate it grows with $N^2$. This rapid growth represents a serious problem when dealing with large systems. We, therefore, will focus our attention in this last term. Let us consider that $H_{LR}$ can be split into two parts

$$H_{LR} = \sum_{|\vec{r}_i - \vec{r}_j| \leq r_c} h_{LR}(\vec{r}_i, \vec{r}_j) + \sum_{|\vec{r}_i - \vec{r}_j| > r_c} h_{LR}(\vec{r}_i, \vec{r}_j). \tag{2}$$

Here $r_c$ is a distance parameter conveniently chosen. Its meaning will be clear in the following. Observe that Eq. (2) is exact, we just rearranged terms. The summation in this first term is to be performed over all pairs inside a volume $\Omega_c = \frac{\Omega}{\Lambda}$, where $\Omega$ is the volume of the system and $\Lambda$ is an integer. To treat the second term we start by enumerating each partition $\Omega_c$, running from $\lambda = 1$ up to $\lambda = \Lambda$ (see Fig. 1(a)–(c)). Inside each box, $\lambda$, we enumerate the particles belonging to that box. Each particle can be identified giving two indexes, $(\lambda, i)$, where $i$ stands for the particle label inside box $\lambda$. Suppose we are computing the contribution of the particle (see Fig. 1). Inside that box we calculate exactly the contribution to Eq. (2). To compute the contribution due to the other cells, $\lambda \neq 1$, we perform an average of all particle contributions inside a given cell with the particle in sight of box $\lambda = 1$ for the remaining cells. To make ourselves clearer let us consider as an example a two dimensional system consisting of $N$ particles inside a box of 'volume' $\Omega$ interacting through a Lennard-Jones (12–6) potential

$$V(i, j) = -4\epsilon \left[ \left( \frac{\sigma}{r_{ij}} \right)^6 - \left( \frac{\sigma}{r_{ij}} \right)^{12} \right], \tag{3}$$

where $\epsilon$ is the minimum of the potential. Reporting to the arrangement shown schematically in Fig. 1, we have chosen a two dimensional ($d = 2$) system with $\Lambda = 25$ and $N = 54$. Extending the definition to a three dimensional system is straightforward. Suppose we have already done the first part of the summation, i.e., the sum inside each cell. For particles outside the cell we approach the interaction by considering the averaged potential inside the cells. To make it clear, consider Fig. 1(a). Cells are labeled from 1 to 25. Inside each cell we enumerated each particle. Suppose we are calculating the interaction between the particle marked $i = 3$ in the cell $\lambda = 1$ and those in cell $\lambda = 14$. Instead of performing the calculation for each particle we consider the averaged interaction due to all particles inside that cell. A *croquis* of this situation is shown in Fig. 1(b), where the open circle represents this average. The process is repeated for each cell $\lambda \neq 1$. The final result is shown in Fig. 1(c). The vector $\bar{\mathbf{R}}_{(1,3),14}$ in Fig. 1(c) is just the arithmetic average of the position vectors of the particles inside cell 14. With those definitions in mind, the interaction potential can be written in an approximate way as

$$V^{CC} \approx -\epsilon \sum_{i,j \, (|\vec{r}_i - \vec{r}_j| \leq r_c)} V(i, j) - \sum_i \sum_\lambda \sum_{\lambda'} \bar{\epsilon}_R \left[ \left( \frac{\sigma}{R_{(i,\lambda),\lambda'}} \right)^6 - \left( \frac{\sigma}{R_{(i,\lambda),\lambda'}} \right)^{12} \right]. \tag{4}$$

Here $\bar{\epsilon}_R = M_\lambda \epsilon$, where $M_\lambda$ represents the number of particles inside cell $\lambda$. In the Lennard-Jones case an upper bound for the error is of order $\mathcal{O}\left((r_c/R_{(i,\lambda),j})^6\right)$. A judicious choice of the size of the cells has to be done in order to minimize the error. As a final remark we observe that the approximation becomes exact in the limit of small $r_c$ ($\rightarrow 0$) and large $r_c$ ($\rightarrow \infty$) cells. In the first case the particle average position inside each cell coincides with the particle position itself, in the later the cell becomes the system so that interactions are exactly calculated.

## 3. The anisotropic dipolar Heisenberg model in two dimensions—a case study

As a case study, we choose to illustrate our approach the two-dimensional anisotropic dipolar Heisenberg (2dADH) model. It is known that it has a transition with a non-divergent specific heat. A behavior like that can easily be confused with

a logarithmic divergence. Besides that, the transition is of the order–disorder type where long-range fluctuations dominate the system and the correlation length goes to infinity. The critical temperature, $T_c$, was determined with great precision [10]. We consider that if we are successful in reproducing those results using the *CC* approach it will give us a clear indication of how far we can go. Let us consider a square lattice, of linear dimensions, $L_x = L_y = L$, where at each site lives a classical Heisenberg spin [10] (see Fig. 2). The spins interact ferromagnetically having an easy axis spin anisotropy and a long-range dipolar interaction. The Hamiltonian describing the system is

$$\mathcal{H} = -J \sum_{i,j} \vec{s}_i \vec{s}_j - A \sum_i (s_i^z)^2 + H_D, \qquad (5)$$

where the first term represents the exchange interaction with the summation running over all nearest neighbor spin pairs and $J$ is an exchange interaction. For $J > 0 \, (<0)$ a ferromagnetic (antiferromagnetic) behavior is expected. The second term represents an anisotropy, which for $A > 0$ favors alignment along the $z$-axis, while for $A < 0$, it favors an in-plane alignment [10,15]. The third term is the long-range dipolar contribution to the Hamiltonian given by

$$H_D = D \sum_{\langle i,j \rangle} \left( \frac{\vec{s}_i \cdot \vec{s}_j}{r_{ij}^3} - 3 \frac{(\vec{s}_i \cdot \vec{r}_{ij})(\vec{s}_j \cdot \vec{r}_{ij})}{r_{ij}^5} \right), \qquad (6)$$

where the sums are now over all pairs of particles ($i \neq j$). We consider periodic boundary conditions. From now on we take $J = 1$. As before we rewrite the long-range interaction in the hamiltonian as

$$H_D \approx H_D^{CC} = D \sum_{i,j \, (|\vec{r}_i - \vec{r}_j| \leq r_c)} \left( \frac{\vec{s}_i \cdot \vec{s}_j}{r_{ij}^3} - 3 \frac{(\vec{s}_i \cdot \vec{r}_{ij})(\vec{s}_j \cdot \vec{r}_{ij})}{r_{ij}^5} \right) \qquad (7)$$

$$+ D \sum_i \sum_\lambda \sum_{\lambda'} \left[ \frac{\vec{s}_i \cdot \vec{m}_{\lambda'}}{R_{(i,\lambda),\lambda'}^3} - 3 \frac{(\vec{s}_i \cdot \vec{R}_{(i,\lambda),\lambda'})(\vec{m}_{\lambda'} \cdot \vec{R}_{(i,\lambda),\lambda'})}{R_{(i,\lambda),\lambda'}^5} \right]. \qquad (8)$$

The first term represents the 'near' contribution of the dipolar interaction. In the second term $\vec{m}_{\lambda'}$ represents the net magnetization inside cell (sum of all spins in the cell) $\lambda'$ and $R_{(i,\lambda),\lambda'}$ is the vector pointing from site $i$ at cell $\lambda$ to the center of the cell labeled $\lambda'$ as shown in Fig. 2. The computational cost to calculate the dipolar interaction, using the above algorithm, becomes proportional to $l^2 + (L/l)^2$ for a square lattice and $(l^3 + (L/l)^3$ for a cubic lattice), where $l = (\Omega_c)^{1/2}$ for a square lattice ($l = (\Omega_c)^{1/3}$ for a cubic lattice). We want to know how good is our approach applied to this specific problem. With this purpose in mind we have used Monte Carlo to study the 2dADH model. We divided the problem in two parts. Firstly, we numerically computed the energy and the magnetization of the system for several values of the dipolar interaction parameter, $D$, and temperature $T$ using: (1) a cutoff, (2) the exact numerical computation of the energies, and (3) the *CC* method. These results were then compared. As a second part of our strategy we used the single histogram method [22,23] to obtain the critical temperature and to show the non-critical behavior of the specific heat. Our results were then compared to those in the literature.

### 3.1. Away from the phase transition

Our first step is the analysis of the energy per spin and the magnetization along the $z$-axis. A second set of results focuses on the dissection of how these quantities are perturbed by performing a side-by-side study of the approximate and exact results during the same simulation run. The runs are for a square lattice size of $28 \times 28$ spins with a cell size of $l = r_c = 7$ for the cutoff case. This use of $r_c = 7$ is more inline with what is being used in the literature. All simulations were performed at a fixed anisotropy coefficient of $A = 2$. Averages were taken over runs of $2.5 \times 10^5$ Monte Carlo steps, which are sufficient for demonstration purposes and for the range of simulated temperatures. In Fig. 3 we show the plots of the energies per spin, $E$, at various temperatures and dipolar coefficients. At all temperatures the *CC* approximation follows the exact results very well. The cutoff case starts to depart from the exact results at the highest dipolar coefficient, except for high $T$, where these approaches give the same results as the long correlations are unimportant. In the more thermodynamically interesting areas of the phase diagram, the cutoff-cell approximation is far superior than the cutoff approximation. For example, at high values of the dipolar coefficient, the *CC* approximation follows the exact values closely while the cutoff approximation poorly reproduces the energies, particularly at high values of the dipolar coefficients. The results for the magnetization along the $z$-axis also provide some useful insight on the approximations. Fig. 4, shows raw Monte Carlo data of the magnetization along the $z$-axis at an intermediate temperature, $T = 0.825$, and at a dipolar coefficient, $D = 0.05$, versus the number of Monte Carlo steps. At this dipolar coefficient and temperature we observe large fluctuations of the values of the magnetization and even field reversal for both the exact and cutoff-cell cases, but these are absent in the cutoff case. Furthermore, generally speaking, the cutoff case shows smaller fluctuations of the magnetization as compared to the exact case. In contrast, the cutoff-cell method preserves the same level of fluctuations of the exact case. This shows that the cutoff-cell approximation retains the long-range memory of the dipolar interaction, which is absent in the cutoff approximation. At values of $d \geq 0.10$
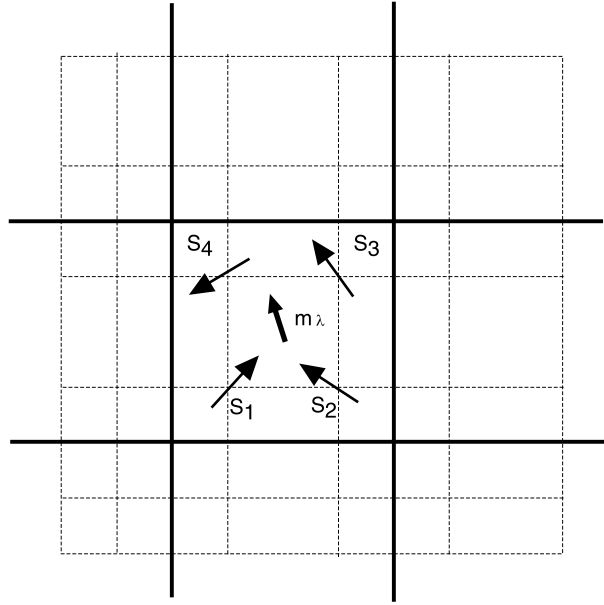
**Fig. 2.** For each of the remaining cells $\lambda > 1$, a net magnetization is computed, given by the sum of all spins belonging to that cell. The spin $i$ centered in cell $\lambda = 1$ then interacts with this net magnetization vector.
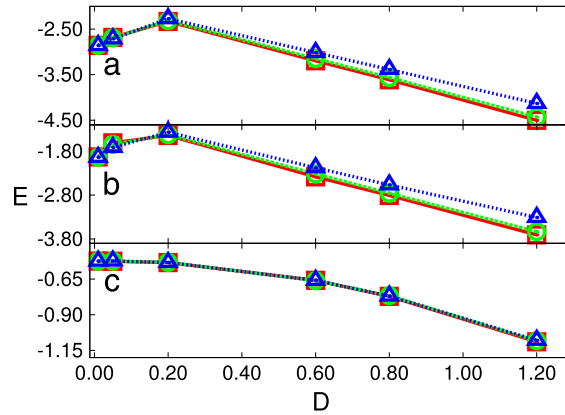


**Fig. 3.** The figure shows the energies per spin for various values of the dipolar coefficient: 0.01, 0.05, 0.2, 0.6, 0.8, 1, and 1.2. Squares represent exact numerical calculations, circles represent the CC method, and triangles represent the cutoff method. Part (a) shows low-temperature results at a value of 0.1. Part (b) is an intermediate temperature of 0.825 and part (c) represents a high-temperature value of 4.

(not shown) the magnetization along the $z$-axis becomes vanishingly small, since the dipolar interaction favors an in-plane alignment of the spins.

We now proceed to show the results of more microscopic quantities, which constitute the second set of quantities as described above. Let us define $\delta E$ as an elemental Monte Carlo energy difference between the trial and current configurations. The average of the absolute energy differences obtained exactly is defined as

$$\langle |\delta E_{\text{Ex}}| \rangle = \frac{\sum_{i=1}^{N_{\text{MCS}}L^2} |\delta E_i^{\text{Ex}}|}{N_{\text{MCS}}L^2}, \tag{9}$$

where $\delta E_i^{Ex}$ is the exact energy difference at every elemental Monte Carlo step and $N_{\text{MCS}}$ represents the number of Monte Carlo steps. Let us also define the mean energy differences between the cutoff-cell approximation and the exact calculation as

$$\langle |\delta E_{\text{Ex-CC}}| \rangle = \frac{\sum_{i=1}^{N_{\text{MCS}}L^2} |\delta E_i^{\text{Ex}} - \delta E_i^{\text{CC}}|}{N_{\text{MCS}}L^2}, \tag{10}$$
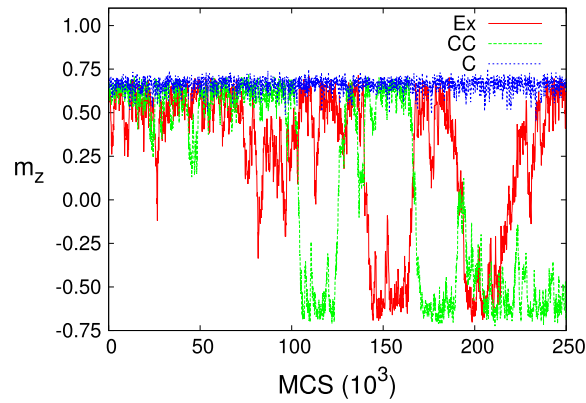
**Fig. 4.** Plots of the magnetization along the *z*-axis for the intermediate temperature of 0.825 versus the number of Monte Carlo steps. Notice that the both the exact and cutoff-cell methods show large fluctuations in the magnetization, including field reversal. These behaviors are absent in the case of the cutoff approximation.
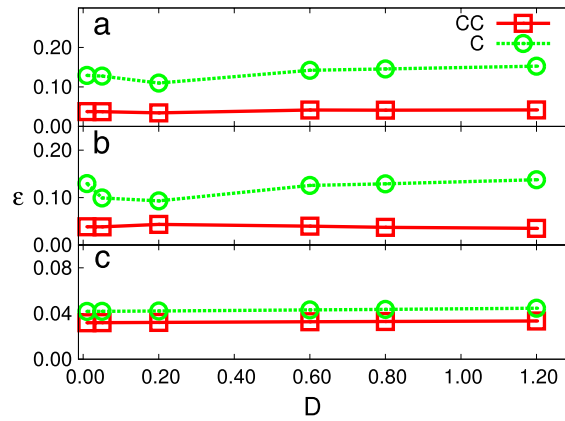


**Fig. 5.** Plot of the ratios, $\epsilon_{CC}$ and $\epsilon_C$ of the difference of the energy differences between the exact values and the cutoff-cell or cutoff energy difference values to the mean exact energy differences, respectively, (please refer to the text) at various values of the dipolar coefficients and for three different temperatures. Please refer to the caption of Fig. 3 for the actual values of the dipolar coefficients and the values of the temperatures in parts (a), (b), and (c).

where $\delta E_i^{CC}$ is the energy difference obtained using the cutoff-cell approximation at a given elemental Monte Carlo step. Similarly, we define the mean energy differences between the cutoff and the exact calculation as

$$\langle |\delta E_{\text{Ex-C}}| \rangle = \frac{\sum_{i=1}^{N_{\text{MCS}}L^2} |\delta E_i^{\text{Ex}} - \delta E_i^{C}|}{N_{\text{MCS}}L^2}, \tag{11}$$

where $\delta E_i^{C}$ represents the cutoff energy difference. In Fig. 5, we show plots of the ratios $\epsilon_{CC} = \langle |\delta E_{\text{Ex-CC}}| \rangle / \langle |\delta E_{\text{Ex}}| \rangle$ and $\epsilon_C = \langle |\delta E_{\text{Ex-C}}| \rangle / \langle |\delta E_{\text{Ex}}| \rangle$ at various temperatures and dipolar coefficients. These ratios probe how off a given approximation is relatively to the exact values, so that the smaller the values the better the approximation. The cutoff approximation gets close to the cutoff-cell approximation values solely at the highest temperature, i.e., when a local sampling is sufficient. In the remaining cases, that is at low and intermediate temperatures, the cutoff-cell approximation is quite superior to the cutoff approximation, with percentage differences into the double digits for most cases. Moreover, the cutoff-cell approximation remains stable within a narrow range of 3.4%–4.15%, while the cutoff ratios are above 9.3% for most cases and drop to about 4.2% for the high-temperature and low dipolar energy values. Though from Fig. 3, the energies per spin seem the same for the exact, cutoff-cell, and cutoff at low values of the dipolar coefficients, Fig. 5 shows that even for these values the cutoff-cell fares better than the cutoff approximation. These results emphasize the consistency of the cutoff-cell approximation across different parameter spaces and ranges, i.e., both in temperature and dipolar coefficient.

Another relevant quantity is the absolute value of the maximum energy difference defined, for the cutoff-cell approximation, by

$$|\delta E_{\text{Max}}^{CC}| = \max\{|\delta E_1^{CC}|, |\delta E_2^{CC}|, \ldots, |\delta E_{N_{\text{MCS}}L^2}^{\text{Ex}}|\}, \tag{12}$$
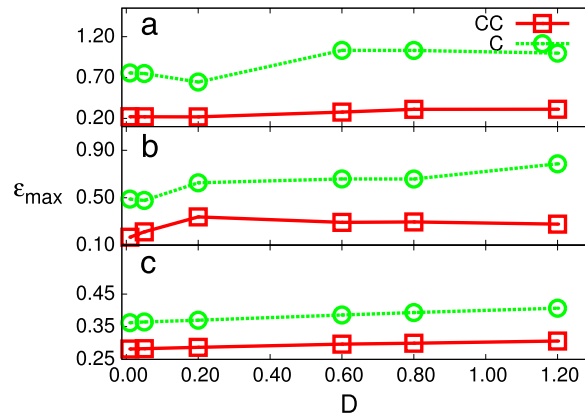
**Fig. 6.** Plot of the ratio of the maximum energy difference to the mean absolute, exact energy difference, $\epsilon_{Max}^{CC}$ and $\epsilon_{Max}^{C}$, respectively, for the cutoff-cell and cutoff approximations for various values of the dipolar coefficients and temperature. The reader is referred to the caption of Fig. 3 for the actual values.
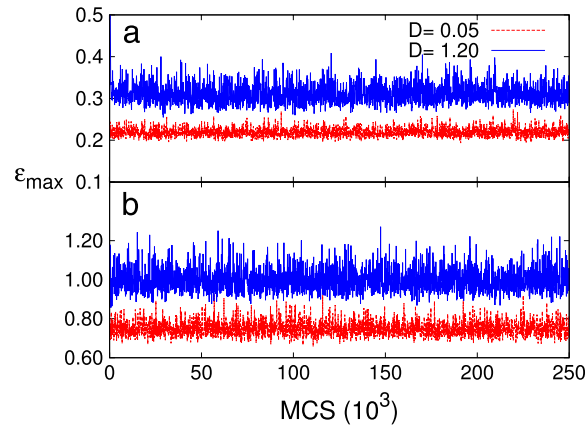


**Fig. 7.** The plots show (a) $\epsilon_{Max}^{CC}$ and (b) $\epsilon_{Max}^{C}$ versus Monte Carlo steps to offer an idea of the fluctuations at $T = 0.1$.

for $N_{MCS}L^2$ elemental Monte Carlo steps, and, similarly, we define

$$|\delta E_{Max}^{C}| = \max\{|\delta E_1^C|, |\delta E_2^C|, \ldots, |\delta E_{N_{MCS}L^2}^C|\}, \tag{13}$$

for the cutoff approximation. This quantity probes how consistent the approximations are over a given number of Monte Carlo steps and the lower the values the better is the approximation. Again, we are interested in ratios of the form $\epsilon_{Max}^{CC} = |\delta E_{Max}^{CC}|/\langle|\delta E_{Ex}|\rangle$ and $\epsilon_{Max}^{C} = |\delta E_{Max}^{C}|/\langle|\delta E_{Ex}|\rangle$ as plotted in Fig. 6. Overall, the deviations are substantially higher in the cutoff than in the cutoff-cell approximation. For example, at the low temperature, the variations in terms of the dipolar coefficient are 21.8%–31.2% for the cutoff-cell approximation, while for the cutoff approximation is 64% to 103%. For the intermediate temperature, the ranges for the cutoff-cell and cutoff approximations are 16.7%–33.8% and 47.7%–78.6%, respectively. Finally, for the high temperature value, the ranges are 28.2%–30.6% and 36.2%–40.7%, respectively. Moreover, the 'instantaneous' deviations of the cutoff approximation can be higher than $\langle|\delta E_{Ex}|\rangle$ as shown in the raw Monte Carlo data of Fig. 7. This does not happen in the case of the cutoff-cell approximation.

### 3.2. Critical properties of the 2dADH model

As our second test to the cutoff-cell method we study the 2dADH model just across a phase transition. The values of the parameters were chosen to reproduce those found in Ref. [10]. In that work the authors have used extensive Monte Carlo calculations to study the planar to paramagnetic phase transition in the 2dADH model. Their results are consistent with an order–disorder phase transition with unusual critical exponents in agreement with previous results for the planar rotator model with dipolar interactions [11]. To apply the CC technique we followed closely Ref. [11]. Initially, we performed an exploratory Metropolis Monte Carlo calculation for several lattice sizes $L = 21, 35, 49, 63, 77, 91, 105,$ and 119, using CC with a cell size of $l = 7$, to determine the region of temperature where the transition is located. Inside this region we have built histograms [22,23] to obtain the maxima of the specific heat and susceptibilities. Using a finite size scaling approach we have obtained the critical temperature from the maximum of the magnetic susceptibility, $\chi = (\langle m^2 \rangle - \langle m \rangle^2)/T$, where
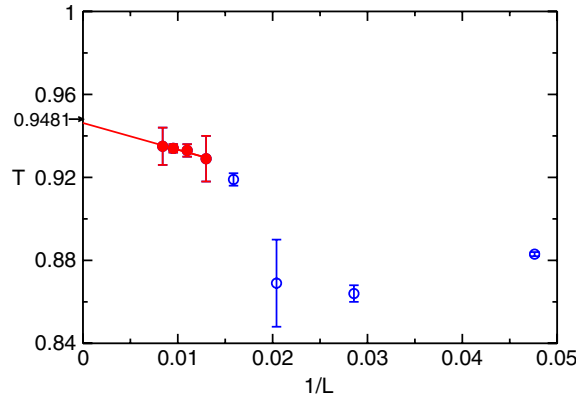
**Fig. 8.** Critical temperature obtained from the maximum of the susceptibility. The blue symbols were not included in the fit. It only includes the largest four lattices (red filled circles) ($L = 77$, 91, 105, and 119). (For interpretation of the references to color in this figure legend, the reader is referred to the web version of this article.)
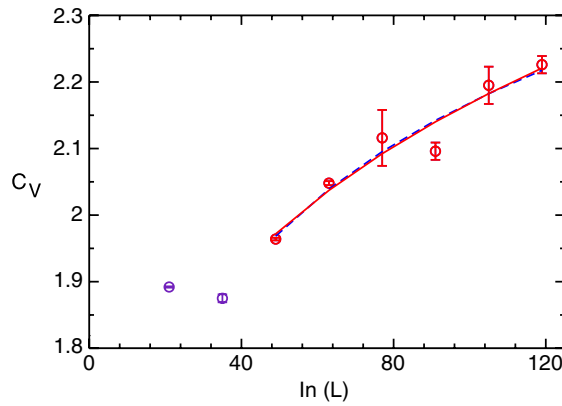


**Fig. 9.** Plot of the maximum of the specific heat for lattice sizes of $L = 21$, 35, 49, 63, 77, 91, 105, and 119 lattice constants. The two smaller lattice sizes (indigo circles) were not used in the two fits, namely, a logarithmic (blue dashed curve) fit and a non-divergent power law (red solid curve). (For interpretation of the references to color in this figure legend, the reader is referred to the web version of this article.)

$m_\alpha = \sum_{i=1}^{N} \sigma_i^\alpha / N$ with $\alpha = \{x, y, z\}$, $N$ the number of spins, and $m = \sqrt{m_x^2 + m_y^2 + m_z^2}$, to be $T_c^{CC} = 0.946(2)$ and the behavior of the specific heat (see Figs. 8 and 9, respectively). The critical temperature agrees very well with that in Ref. [10], $T_c = 0.9481(1)$. For the specific heat, given by $c_V = (\langle E^2 \rangle - \langle E \rangle^2)/NT$, we found that it is compatible with a non-divergent behavior, the same conclusion found in Ref. [10]. We have to pay attention to the small lattice results differences found in Ref. [10] and this work. For small lattices we do not expect that the approach could work well since we loose the long range fluctuations of the system. In this case, the susceptibilities cannot follow the exact values.

Now, as the system size increases, the cells further away from site $i$ have an interaction closer to the exact value, since the vector connecting site $i$ to the center of any other such cell deviates less and less from the position vectors of the individual spins inside the cell. Therefore, the *CC* method becomes more accurate as the system size increases for a given cell size, $l$. For large system sizes, the calculation of the long-range term becomes quite accurate, so the dynamics of the larger systems sizes approach that of the exact numerical calculation. This was the reason why we had to discard the smaller systems sizes, but the largest lattice showed the expected convergence.

## 4. Concluding remarks

We have introduced a general novel approach to compute long-range interactions. The method can save a lot of computer time since it performs an average over far cell interactions. When applied to the anisotropic dipolar Heisenberg model in two dimensions the results obtained compares remarkably well with exact calculations using Ewald summation.

The cutoff-cell approach becomes exact in the limit of large and small cell sizes. At fixed cell-size, the method approaches the exact results as the system size increases. The computational effort of the method scales with the number of cells defined on the lattice at each Monte Carlo elemental update step. It is, therefore, possible to study systems as large as $4 \times 10^4$ spins on a single processor of present day desktop computers. As a remark, we would stress that although we applied the approximation to Monte Carlo, it should work well in any molecular dynamics calculation.

## Acknowledgments

## References

[1] D. Frenkel, B. Smit, Understanding Molecular Simulation: From Algorithms to Applications, Academic Press, 2002.
[2] D.M. York, T,A. Darden, L.G. Pedersen, The effect of long-range eletrostatic interactions in simulations of macromolecular crystals: a comparison of the Ewald and truncated list methods, J. Chem. Phys. 99 (1993) 8345.
[3] U. Essmann, L. Perera, M.L. Berkowitz, T. Darden, H. Lee, L.G. Pedersen, A smooth particle mesh Ewald method, J. Chem. Phys. 103 (1995) 8577.
[4] T. Darden, D. York, L. Pedersen, Particle mesh Ewald: an $N \cdot \log(N)$ method for Ewald sums in large systems, J. Chem. Phys. 98 (1993) 10089.
[5] L. Greengard, V. Rokhlin, A fast algorithm for particle simulations, J. Comput. Phys. 73 (1987) 325–348.
[6] L. Greengard, V. Rokhlin, A fast algorithm for particle simulations, J. Comput. Phys. 135 (1997) 280–292.
[7] R. Hockney, J.W. Eastwood, Computer Simulation Using Particles, CRC Press, 2010.
[8] B.A. Luty, I.G. Tironi, W.F. van Gunsteren, Lattice-sum methods for calculating electrostatic interactions in molecular simulations, J. Chem. Phys. 103 (1995) 3014.
[9] M. Rapini, R.A. Dias, B.V. Costa, Phase transition in ultrathin magnetic films with long-range interactions: Monte Carlo simulation of the anisotropic Heisenberg model, Phys. Rev. B 75 (2007) 014425.
[10] L.A.S. Mól, B.V. Costa, The phase transition in the anisotropic Heisenberg model with long-range dipolar interactions, J. Magn. Magn. Mater. 353 (2014) 11.
[11] L.A.S. Mól, B.V. Costa, Anisotropic Heisenberg model with dipolar interactions: Monte Carlo simulations of the planar-to-paramagnetic phase transition in a bilayer system, Phys. Rev. B 79 (2009) 054404.
[12] L.A.S. Mól, B.V. Costa, Phase transition in the two-dimensional dipolar rotator model, J. Phys.: Condens. Matter. 22 (2010) 046005.
[13] A. Aguado, P.A. Madden, Ewald summation of electrosatic multipole interactions up to the qruadupolar level, J. Chem. Phys. 119 (2003) 7471.
[14] N.G. Almarza, E. Lomba, C. Martín, A. Gallardo, Demixing in binary mixuteres of apolar and dipolar hard spheres, J. Chem. Phys. 129 (2008) 234504.
[15] C. Santamaria, H.T. Diep, Dipolar interactions in magnetic thin films: perpendicular to in-plane ordering transition, J. Magn. Magn. Mater. 212 (2000) 23.
[16] A. Ashok, D. Vasileska, O.L. Hartin, S.M. Goodnick, Electrothermal Monte Carlo simulation of GaN HEMTs including electron–electron interactions, IEEE Trans. Electron Devices 57 (2010) 562.
[17] W. Lee, U. Ravaioli, in Ref. [24].
[18] K. Matyash, R. Schneider, R. Ikkurthi, L. Lewerentz, A. Melzer, $P^3M$ simulations of dusty plasmas, Plasma Phys. Control. Fusion 52 (2010) 124016.
[19] A.M. Abu-Labdeh, J.P. Whitehead, K. De'Bell, A.B. MacIsaac, Phase behavior of antiferromagnetic ultrathin magnetic films, Phys. Rev. B 65 (2001) 024434.
[20] A.M. Abu-Labdeh, A.B. MacIsaac, K. De'Bell, Effects of a perpendicular magnetic field in the dipolar Heisenber model with dominant exchange interaction, J. Phys.: Condens. Matter. 23 (2011) 296005.
[21] S.A. Leonel, I.A. Marques, P.Z. Coura, B.V. Costa, A model for vortex formation in magnetic nanodots, J. Appl. Phys. 102 (2007) 104311.
[22] M.E.J. Newman, G.T. Barkema, Monte Carlo Methods in Statistical Physics, Clarendon Press, Oxford, 1999.
[23] A.M. Ferrenberg, R.H. Swendsen, New Monte Carlo technique for studying phase transitions, Phys. Rev. Lett. 61 (1988) 2635.
[24] G. Baccarani, M. Rudan, SISPAD 2010—15th International Conference on Simulation of Semiconductor Processes and Devices, IEEE, 2010.